

Optimization of a cationic dye removal by a chemically modified agriculture by-product using response surface methodology: biomasses characterization and adsorption properties

Ahmed Amine Azzaz^{1,2} · Salah Jellali¹ · Hanene Akrouit¹ · Aymen Amine Assadi³ ·
Latifa Bousselmi¹

Received: 31 May 2016 / Accepted: 12 September 2016 / Published online: 10 October 2016
© Springer-Verlag Berlin Heidelberg 2016

Abstract The present study investigates the alkaline modification of raw orange tree sawdust (ROS) for an optimal removal of methylene blue (MB), as a cationic dye model, from synthetic solutions. The effects of operating parameters, namely, sodium hydroxide (NaOH) concentrations, ROS doses in NaOH solutions, stirring times, and initial MB concentrations on dye removal efficiency, were followed in batch mode. The process optimization was performed through the response surface methodology approach (RSM) by using Minitab17 software. The results showed that the order of importance of the followed parameters was NaOH treatment concentrations > stirring times > initial MB concentrations > ROS doses in NaOH solutions. The optimal experimental conditions ensuring the maximal MB removal efficiency was found for a NaOH treatment concentration of 0.14 M, a stirring time of 1 h, a ROS dose in NaOH solutions of 50 g L⁻¹, and an initial MB concentration of 69.5 mg L⁻¹. Specific analyses of the raw and alkali-treated biomasses, e.g., SEM/

EDS and XRD analyses, demonstrated an important modification of the crystalline structure of the wooden material and a significant increase in its surface basic functional groups. Kinetic and isotherm studies of MB removal from synthetic solutions by ROS and the alkali-treated material (ATOS) showed that for both adsorbents, the pseudo-second-order and Langmuir model fitted the best the experimental data, respectively, which indicates that MB removal might be mainly a chemical and a monolayer process. Furthermore, thanks to the chemical modification of the ROS, the MB maximal uptake capacity has increased from about 39.7 to 78.7 mg g⁻¹. On the other hand, due to the competition phenomenon, the coexistence of MB and Zn(II) ions could significantly decrease the MB removal efficiency. A maximal decrease of about 32 % was registered for an initial Zn(II) concentration of 140 mg L⁻¹. Desorption experiments undertaken at natural pH (without adjustment: pH = 6) and with different NaCl concentrations emphasized that the adsorbed MB

Responsible editor: Vitor Pais Vilar

Electronic supplementary material The online version of this article (doi:10.1007/s11356-016-7698-6) contains supplementary material, which is available to authorized users.

✉ Salah Jellali
salah.jellali@certe.mrt.tn

Ahmed Amine Azzaz
ahmedamine.azzaz@certe.mrt.tn

Hanene Akrouit
hanene.akrouit@yahoo.com

Aymen Amine Assadi
aymen.assadi@ensc-rennes.fr

Latifa Bousselmi
latifa.bousselmi@certe.mrt.tn

- ¹ Wastewaters and Environment Laboratory, Water Research and Technologies Center, BP 273, 8020 Soliman, Tunisia
- ² Faculty of Sciences of Bizerte, University of Carthage, 7000 Jarzouna, Tunisia
- ³ Laboratory of Chemical Sciences of Rennes Sciences—Chemical and Process Engineering team, MRU 6226 ICSR, ENSCR-11, Allée de Beaulieu, 508307-35708 Rennes, France

could be significantly desorbed from both the tested materials, offering their possible reuse as efficient adsorbents. All these results confirmed that NaOH-treated orange tree sawdust could be considered as an efficient, economic, and ecological alternative for the removal of cationic dyes from industrial wastewaters.

Keywords Orange tree sawdust · Chemical modification · Methylene blue · Response surface methodology · Sorption characteristics

Introduction

The quick urbanization induced by growing industrial activities has caused an increasing demand in energy and natural resources. Such rapid development was accompanied with an increase of the generated industrial effluents containing toxic substances that are sometimes discharged in natural water streams without adapted treatment (Akrouit et al. 2015). These effluents could alter the fauna and flora ecosystem and raise the concern about the human health. One of the most important compounds contained in these industrial effluents are dyes. These chemical substances are widely used in various industrial sectors, since yearly, about 700,000 t are produced and 100 t are thrown in water streams without prior appropriate treatment (Yagub et al. 2014). Wastewaters containing dyes could significantly deteriorate the water bodies' quality due to the eutrophication phenomenon characterized by excessive oxygen depletion as algae decay. Even at low concentrations, human exposure to some dyes could lead to serious health aggravations due to their possible carcinogenic and mutagenic properties (Rafatullah et al. 2010).

Many techniques have been tested and used for the treatment of wastewaters loaded with dyes such as membrane separation (Soniya and Muthuraman 2013), ozonation (Al jibouri et al. 2015), anodic oxidation (Akrouit et al. 2015), and biological degradation (Ding et al. 2016). However, these methods are usually characterized by an important generation of toxic by-products and high investment, operational, and maintenance costs due to huge consumption of energy and chemicals. Adsorption onto low-cost materials has emerged this last decade as an interesting alternative for dye removal from industrial effluents due to their confirmed removal efficiency, insignificant costs, and abundance. An important number of mineral and organic low-cost adsorbents were reported in scientific literature for the removal of dyes such as raw and modified clays, coal ash, tea wastes, activated carbon, olive tree pruning, and hazelnut shell (Rafatullah et al. 2010). Adsorption onto organic lignocellulosic

materials, namely, hardwood tree sawdust, was recognized to be among the most efficient by-products for dye removal from wastewaters, due to their important outer and inner surface and the presence of various functional groups leading to the fixation of dye molecules (Kalavathy et al. 2009).

In order to improve the sawdust's efficiencies in removing dyes and other inorganic pollutants from industrial effluents, various chemical and/or thermal modification of these raw lignocellulosic studies have been tested. They included the use of various acids (Calero et al. 2013; Kalavathy et al. 2009), bases (Djilali et al. 2012; Azzaz et al. 2015), salts (Batziar and Sidiras 2007), and pyrolysis (Jellali et al. 2016). These studies have reported that the modified lignocellulosic materials presented relatively higher pollutant removal efficiencies compared to the raw ones. This finding was attributed mainly to the improvement of the surface properties (specific surface area, microporosity, pH of zero point charge) as well as the enrichment with various functional groups (Nazari et al. 2016). However, the majority of these studies did not present a detailed characterization of the modified biomasses, missed the investigation on the involved mechanisms, and did not assess accurately the effect of combined pollution including both dyes and inorganic pollutants such as metals. Furthermore, these studies were usually performed for fixed experimental conditions and the effect of a given variable was assessed when keeping the others constant (Jellali et al. 2016). Since the individual variables could influence each other and the optimal value of one of them can depend on the values of the others, the need for the use of new tools/approaches, permitting the optimization of the material modification and dye adsorption process through a simultaneous study of the effect of several parameters, has been pointed out by several authors (Kalavathy et al. 2009; Pavlović et al. 2014). In this context, the use of design of experiment (DOE) figured as an interesting mathematical solution for a better understanding of the complex interactions that could occur between the chosen parameters during the modification process and to determine the optimal conditions for a maximal desired response (Ghaedi et al. 2015).

The main objectives of this study were (i) to determine the optimal experimental conditions for the impregnation of raw orange tree sawdust (ROS) by alkaline solutions in order to guarantee the best removal efficiencies of MB from aqueous solutions, (ii) to assess the effect of the chemical modification onto the orange tree sawdust physical-chemical properties through specific analyses, (iii) to evaluate the MB removal efficiency by both ROS and alkali-treated orange tree sawdust (ATOS) under various experimental conditions, (iv) to assess the impact of the coexistence of MB and Zn(II) on the dye removal

efficiency, and finally, (v) to gain a better understanding of the possible mechanisms involved in the adsorption of dye by these biomasses.

Materials and methods

Raw biomass preparation

Raw orange tree sawdust (ROS) was collected from a local farm in the city of Menzel Bouzelfa (Nabeul, Tunisia). This material was washed several times with tap water in order to remove the contained impurities, and then sieved using mechanical sieve shakers (Retsch, Haan, Germany). Only the fraction with particle diameters lower than 2 mm was selected, dried in an oven at 60 °C for 24 h, and stored in bags for further use.

Chemical modification of the biomass

In this study, an alkali treatment of ROS by various NaOH solution concentrations was performed since this reagent has previously demonstrated interesting MB removal efficiencies but for relatively high alkali concentration (1 M) (Djilali et al. 2012; Azzaz et al. 2015). The preparation of the modified orange tree sawdust was established by the experimental design given in Table 1. The chemical modification was performed through the mixing of a certain amount of ROS with 400 mL of a sodium hydroxide (NaOH) solution at a given molar concentration. The mixture was stirred for a given time at 900 rpm using a “Thermolyne” magnetic stirrer. The biomass was then filtered through cellulosic filtering paper and washed abundantly with distilled water until the rinsing pH remained constant. The collected sawdust was then dried overnight at 60 °C by using an electric oven (Memmert, Germany). The resulting material was stocked for ulterior MB adsorption tests in batch mode.

Experimental design

Central composite rotatable design (CCRD), which was the subject of many studies conducted for fitting response surface design of experiments (Kalavathy M. et al. 2009; Das et al. 2014; Ghaedi et al. 2015), was used for the optimization of the orange tree sawdust modification process. To assess the effect of the experimental parameters on the MB removal yields (Y (%)), four independent variables were followed (Table 1): NaOH treatment concentration (X_1 ; Mol L⁻¹), dose of ROS in the NaOH solutions (X_2 ; g L⁻¹), stirring time (X_3 ; min), and MB initial concentration (X_4 ; mg L⁻¹). The used mathematical and statistical approaches as well as the theoretical considerations for the optimization process were widely described in literature (Ghaedi et al. 2015; Kalavathy et al. 2009).

Table 1 Level of the factors used for the study of MB adsorption by the chemically modified orange tree sawdust using the central composite design approach (X_1 : NaOH concentration (mol L⁻¹), X_2 : dose of ROS in NaOH solutions (g L⁻¹), X_3 : stirring time (min), X_4 : MB initial concentration (mg L⁻¹), $\pm\alpha$: axial points)

	($-\alpha = -2$)	Low (-1)	Central (0)	High ($+1$)	($+\alpha = 2$)
X_1	0.02	0.06	0.1	0.14	0.18
X_2	25	50	75	100	125
X_3	0	30	60	90	120
X_4	60	80	100	120	140

For the MB adsorption experiments, 0.1 g of the chemically modified adsorbent under specific conditions (see Table 1) was added to 100 mL of an MB solution with an appropriate initial concentration at a speed of 400 rpm. The contact time was fixed to 3 h based on preliminary kinetic experiments and was judged sufficient to reach an equilibrium state characterized by stable residual MB concentrations (Azzaz et al. 2015).

At equilibrium, the amount of the adsorbed MB (q_e (mg g⁻¹)) and the corresponding removal yield (Y_e (%)) were calculated using the following equations:

$$q_e = \frac{(C_0 - C_e) \times V}{M} \tag{1}$$

$$Y_e(\%) = \frac{(C_0 - C_e)}{C_0} \times 100 \tag{2}$$

where C_0 and C_e are the dye concentrations initially and at equilibrium, respectively (mg L⁻¹), M is the used modified adsorbent mass (g) and V is the MB solution volume (L).

Characterization of the raw and modified sawdust

The ROS and ATOS were physicochemically characterized by using several apparatus and analyses. First of all, the corresponding particle size distribution was performed using a laser granulometric device (Mastersizer 2000 device, Malvern, UK). Then, their composition in terms of moisture, lignin, cellulose, and hemicellulose were assessed according to experimental protocol given by Das et al. (2014) and thermogravimetric analyses by using a Q500 thermogravimetric analysis (TGA) unit (TA Instruments, Delaware, USA). Afterward, a high-resolution microscopy analysis was performed using a JSM 7100F scanning electron microscope (Jeol, Tokyo, Japan) to study the morphological modifications that occurred on the biomass surface after the chemical treatment of ROS. The scanning electron microscope (SEM) system was coupled with an energy-dispersive X-ray spectroscope (EDS) (Oxford Instruments, Oxfordshire, UK) in order to determine the atomic composition of the studied adsorbents. The ROS and ATOS were also analyzed by X’Pert PRO MPD X-ray diffractometer (PANalytical, Almelo, Netherlands) for crystalline phase identification. The peaks were defined using

the X'Pert High Score Plus software. On the other hand, to determine the surface functional groups on both ROS and ATOS, Boehm titration was performed by applying the experimental method presented in literature as follows (Boehm 2002): 1.5 g of the solid matrix was placed in round-bottom flasks containing 50 mL of 0.1 M of NaOH, Na₂CO₃, NaHCO₃, and HCl solutions, assuming that NaOH was used to neutralize phenolic, lactonic, and carboxylic acids; sodium carbonate was added to neutralize the carboxylic and lactonic groups; sodium bicarbonate was used to neutralize the carboxylic acids; and chlorhydric acid was added to neutralize the basic groups. The samples were stirred for 24 h at 200 rpm at room temperature (20 ± 2 °C). The mixture was then centrifuged at 3000 rpm and filtered using 0.45-µm membranes. Bases were back-titrated with 0.05 M HCl solutions and HCl aliquots were back-titrated with 0.05 M NaOH solutions. The point of null net charge for the studied biomasses, pH_{zpc}, was determined for ROS and ATOS according to the methodology given by Wan Ngah and Hanafiah (2008).

MB and zinc solution preparation and analyses

The used dye, methylene blue (C₁₆H₁₈ClN₃S, MW = 319.852 g mol⁻¹, purity = 98 %) was obtained from PANREAC (PanreacQuimica S.A., Barcelona, Spain). The desired MB solutions at given concentrations were prepared by diluting a stock dye solution at a concentration of 1 g L⁻¹ with distilled water. The MB removal from aqueous solutions by the used adsorbents was determined by measuring the progress in time of the measured absorbance at 664 nm by using a UV–Vis spectrophotometer (Thermo-Spectronic UV1, Thermo Fischer Scientific, USA).

Zinc nitrate (Zn(NO₃)₂·6H₂O, MW = 297.49 g mol⁻¹, purity ≥98 %), acquired from Sigma Aldrich (Saint Louis, USA), was used in the batch combined pollution experiment. A stock solution of Zn(NO₃)₂ with a concentration of 1 g L⁻¹ was prepared, and further dilutions with distilled water were performed in order to obtain the desired concentrations of zinc. The Zn(II) concentrations were measured by using an atomic absorption spectrometry unit (Perkin Elmer, Massachusetts, USA).

It is worth mentioning that each analysis point reported in this study was an average of three independent parallel sample solutions. Triplicate tests showed that the standard deviation of the results was ±3 %.

MB kinetic and isotherm adsorption studies

The MB removal kinetic from aqueous solutions by both ROS and ATOS was followed at various times between 1 and 240 min for an initial dye concentration of 69.5 mg L⁻¹, an adsorbent dose in MB solutions of 1 g L⁻¹, an initial aqueous pH of 6, and at temperature of 20 ± 2 °C.

The MB adsorption at equilibrium was investigated for dye concentrations varying between 10 and 50 mg L⁻¹ for ROS and

between 40 and 100 mg L⁻¹ for ATOS with constant contact time of 3 h. These experiments were performed for fixed adsorbent dosages, aqueous pH, and temperature of 1 g L⁻¹, 6.0, and 20 ± 2 °C, respectively.

To fit the kinetic and at equilibrium experimental data, several theoretical models were employed in literature (Jellali et al. 2011b). In this study, the most common ones were used for the kinetic prediction (pseudo-first order, pseudo-second order, film, and intraparticle diffusion models) and for isotherm assessment (Langmuir, Freundlich, and Dubinin–Radushkevich models; Azzaz et al. 2015). The corresponding original and linearized equations as well as the related plots are depicted in Table 2.

The concordance between the theoretical kinetic and isotherm data and the experimental ones was apprehended through the calculus of average percentage errors (APE):

$$APE_{\text{kinetic}}(\%) = \frac{\sum \left[\frac{(q_{t,\text{exp}} - q_{t,\text{calc}})}{q_{t,\text{exp}}} \right]}{N} \times 100 \quad (3)$$

$$APE_{\text{isotherm}}(\%) = \frac{\sum \left[\frac{(q_{e,\text{exp}} - q_{e,\text{calc}})}{q_{e,\text{exp}}} \right]}{N} \times 100 \quad (4)$$

where $q_{t,\text{exp}}$ and $q_{t,\text{calc}}$ (mg g⁻¹) are the experimental and the calculated adsorbed amounts at a given time “ t ”, respectively, $q_{e,\text{exp}}$ and $q_{e,\text{calc}}$ (mg g⁻¹) are the experimental and the calculated adsorbed amounts at equilibrium, respectively, and N is the number of the experimental runs.

Effect of initial solution pH

Initial solution pH impact on the MB removal by ROS and ATOS was carried out for values of 3, 5, 6, 9, and 11. These experiments were performed for fixed adsorbent dosages, aqueous MB concentration, and temperature of 1 g L⁻¹, 69.5 mg L⁻¹ and 20 ± 2 °C, respectively.

Adsorption mechanisms investigation

In order to investigate the importance of ionic exchange mechanism during the MB adsorption process by ROS and ATOS, the release of the main cations (sodium, magnesium, calcium, ammonium, and potassium) was followed for blank solutions (distilled water without MB) and for solutions with a fixed MB concentration of 69.5 mg L⁻¹ in batch mode. These cations were measured by using a Metrohm ionic chromatograph (Metrohm, Herisau, Switzerland). The experiments were performed for 0.1 g of biomasses, 100 mL of solution volume, pH of 6.0, a contact time of 180 min (equilibrium state), and a temperature of 20 ± 2 °C.

Effect of competition with zinc ions

In order to simulate a real textile effluent that generally contains organic pollution combined with heavy metals (Kyzas et al.

Table 2 Used models for the kinetic and isotherm studies

Kinetic models			
Model	Equation	Linear forms	Reference
Pseudo-first order	$\frac{dq_t}{dt} = k_1(q_e - q_t)$	$\ln(q_e - q_t) = \ln q_{e1} - k_1 t$	Jellali et al. (2011b)
Pseudo-second order	$\frac{dq_t}{dt} = k_2(q_e - q_t)^2$	$\frac{t}{q_t} = \frac{1}{k_2 q_e^2} + \frac{1}{q_{e1}} t$	
Film diffusion		$\frac{q_t}{q_e} = 6 \left(\frac{D_f}{\pi a^2} \right)^{1/2} \sqrt{t}$	
Intraparticle diffusion		$\ln \left(1 - \frac{q_t}{q_e} \right) = \ln \left(\frac{6}{\pi^2} \right) - \left(\frac{D_{ip} \pi^2}{a^2} \right) t$	
Isotherm models			
Model	Equation	Linear forms	Reference
Langmuir	$q_e = \frac{q_{max,L} K_L C_e}{1 + K_L C_e}$	$\frac{C_e}{q_e} = \frac{1}{K_L q_m} + \frac{1}{q_m} C_e$	Azzaz et al. (2015)
Freundlich	$q_e = K_F C_e^{1/n}$	$\ln C_e = \ln K_F + \frac{1}{n} \ln C_e$	
Dubinin–Radushkevich	$q_e = q_m \exp [-\beta \varepsilon^2]$	$\ln q_e = \ln q_m - \beta \varepsilon^2$	

(min^{-1}) and k_2 ($\text{g mg}^{-1} \text{min}^{-1}$) pseudo-first- and pseudo-second-order kinetic constants, respectively, q_{e1} and q_{e11} (mg g^{-1}) pseudo-first- and pseudo-second-order theoretical adsorbed amounts of MB, respectively, D_f and D_{ip} ($\text{m}^2 \text{sec}^{-1}$) diffusion film and intraparticle diffusion constants, respectively, K_L (L mg^{-1}) and K_F ($\text{mg}^{1-(1/n)} \text{L}^{1/n} \text{g}^{-1}$) Langmuir and Freundlich constants, respectively, n adsorption intensity, β Dubinin–Radushkevich isotherm constant ($\text{mol}^2 \text{kJ}^{-2}$), ε potential energy constant

2015), the effect of a combined MB-zinc pollution on dye removal efficiency by ATOS was investigated. Therefore, the MB adsorption was studied at zinc concentrations of 30, 70, and 140 mg L^{-1} . During these studies, the used MB concentration, ATOS dosage, initial solution pH, and temperature were fixed to 69.5 mg L^{-1} , 1 g L^{-1} , 6.0, and 20 ± 2 °C, respectively. The contact time was fixed to 3 h which is judged sufficient to reach an equilibrium state.

MB desorption experiments

MB desorption efficiency from preloaded ROS and ATOS for an aqueous concentration of 69.5 mg L^{-1} was performed using various sodium chloride solutions. The use of NaCl was chosen as a desorbent for its low cost and its satisfactory dye recovery efficiencies according to preliminary fixed bed column experiments (data not shown). During these experiences, masses of 0.1 g of the MB loaded materials were stirred with 100 mL of distilled water at different NaCl concentrations of 0.05, 0.1, 0.25, 0.5, and 1 M at 20 °C for 2 h. The desorbed MB amounts q_d (mg g^{-1}) and the corresponding desorption yields were calculated as follows:

$$q_d = \frac{C_d}{M} \times V \tag{5}$$

$$Y_d(\%) = \frac{q_d}{q_e} \times 100 \tag{6}$$

where C_d is the MB desorbed concentration (mg L^{-1}) and q_e is the adsorbed amount of dye at equilibrium (mg g^{-1}).

Results and discussion

Optimization of the sawdust modification using RSM approach

Fitting the design model

In the present study, five levels of CCRD with four variables (NaOH treatment concentration, ROS dose in NaOH solutions, stirring time, and initial MB concentration) were used as DOE model. A total of 31 experiments were carried out for the establishment of the design. To determine the statistical significance of the different coefficient terms, namely, the linear, square, and interaction patterns, as well as the difference between observed and calculated MB removal yield and ANOVA test were established and the results are shown in Tables S1 and S2. Afterward, in order to emphasize the statistical importance of each variable, the variance distribution (F) was compared to the probability of the studied parameters. In general, the coefficients presenting high Fischer’s test coefficients “ F ” values with low probability “ P ” designate an important significance of the regression model (Pavlović et al.

2014). In our study, the confidence level of 95 % was set for the experimental design ($p < 0.05$).

The empirical regression model between the tested variables and the response is presented by the following Eq. (7):

$$\begin{aligned}
 Y = & 190.748 + 243.671X_1 - 0.469X_2 \\
 & + 6.508X_3 - 2.169X_4 - 115.48X_1^2 \\
 & + 0.002X_2^2 - 0.77X_3^2 + 0.007b_{44}X_4^2 \\
 & + 0.434X_1X_2 - 21.95X_1X_3 \\
 & + 0.199X_1X_4 - 0.024X_2X_3 - 0.00023X_2X_4 \\
 & + 0.083X_3X_4
 \end{aligned} \quad (7)$$

Positive and negative signs in the latter equation indicated synergistic and antagonist effects of the variables, respectively. The lack of fit (LOF), as a data variation criteria, presents the non-suitability of the codified model for the fitting of the experimental values (Tehrani and Zare-Dorabei 2016). The probability of the LOF for the present study was determined to be about 0.003 ($p < 0.05$) (Table S1), which indicates a good concordance between the experimental and the predicted MB removal efficiencies. Moreover, ANOVA results showed that the linear effects of NaOH chemical concentration X_1 , ROS dose in NaOH solutions X_2 , stirring time X_3 , and initial methylene blue concentration X_4 presented low p values and were estimated to be statistically substantial. Furthermore, the overall probability for linear parameters was estimated to be 0.011 ($p < 0.05$) and indicates a high correlation between experimental and the calculated MB removal yields.

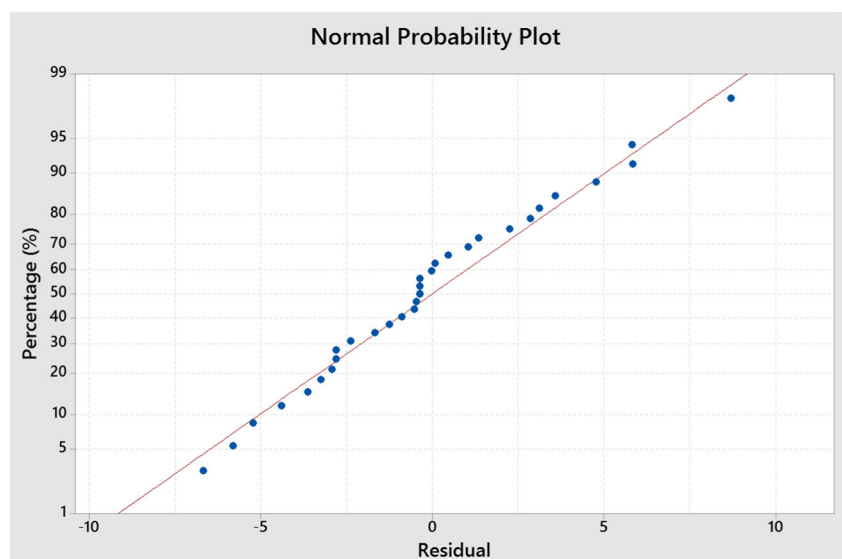
However, in the case of the quadratic variation, the experimental conditions seem to be less significant due to the increase of p value and the decrease of F -values (Table S1). In fact, only the NaOH concentration X_1^2 and initial dye concentration X_4^2 were significant ($p < 0.05$), in opposition to ROS dose in NaOH solutions X_2^2 and stirring time X_3^2 where the p values exceeded 0.05 (Table S1). Similarly, in the case of a two-way interaction condition, all the effects were insignificant, since they presented high p values ($p > 0.05$) and low F -values (Table S1). These findings suggest that the chosen parameters are characterized with an antagonist behavior in the case of a simultaneous variation, thus limiting the MB uptake onto the modified sawdust. Similar results were observed by Ghaedi et al. (2015) when they investigated the simultaneous removal of MB and lead by walnut wood-activated carbon.

Considering the latter results, the empirical regression model could be simplified as follows:

$$\begin{aligned}
 Y = & 190.748 + 243.671 X_1 - 0.469 X_2 \\
 & + 6.508 X_3 - 2.169 X_4 - 115.48 X_1^2 + 0.007 X_4^2
 \end{aligned} \quad (8)$$

ANOVA results for the chosen response parameters showed high determination coefficients ($R^2 = 0.973$ and adjusted $R^2 = 0.955$), which confirmed the good fitting of the elaborated design to theoretical data. Besides, the normal probability plot (Fig. 1) indicated the existence of a clear linearity between the experimental data and those determined by the model with a small deviation amount around the mean. This finding indicates a normal error distribution and a well fitting of the model (Ghaedi et al. 2015).

Fig. 1 Normal probability plot between residual and error percentage



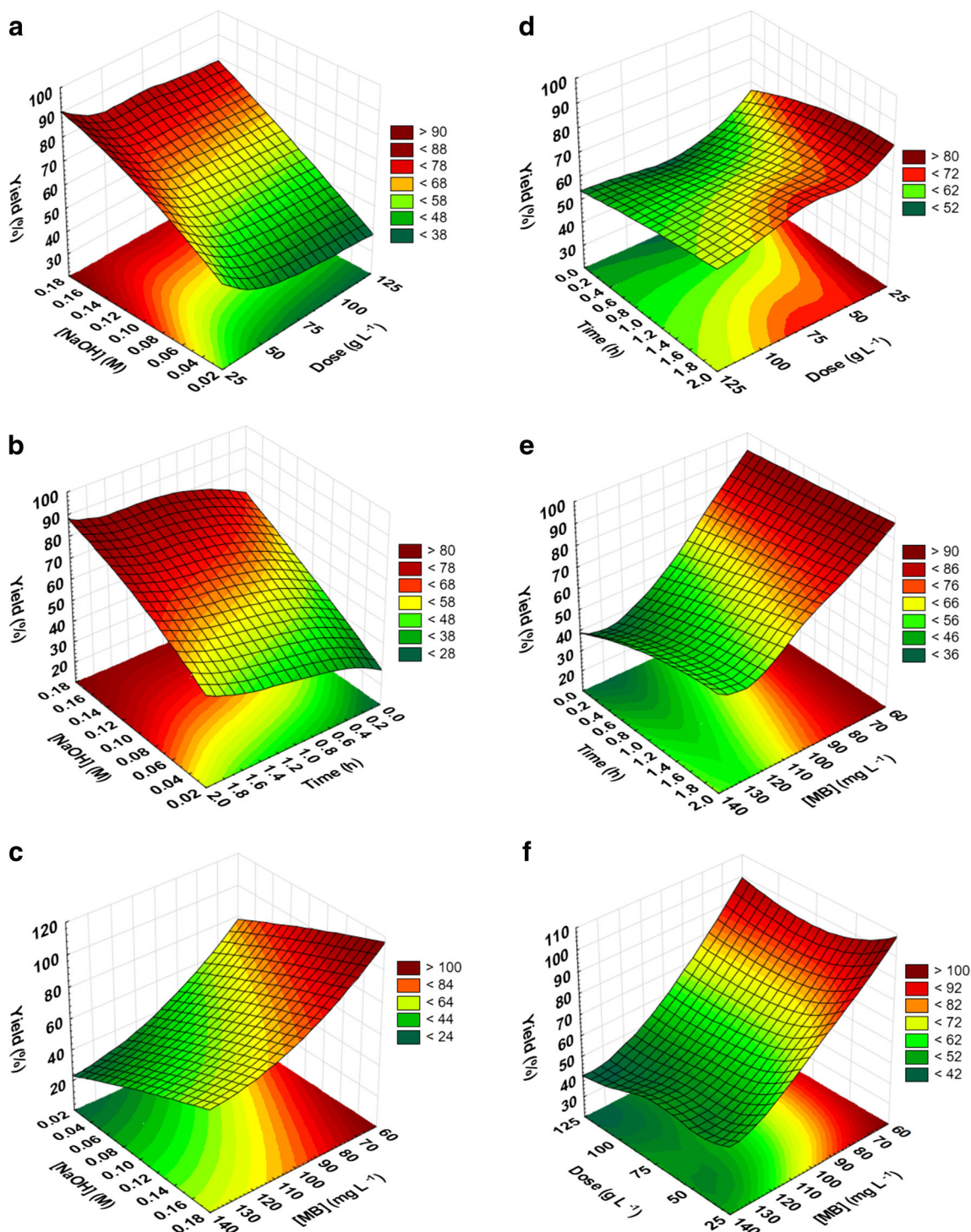


Fig. 2 3D response surface for the 2⁴central composite designs (NaOH chemical concentration: X₁, ROS dose in NaOH solutions: X₂, stirring time: X₃, and initial methylene blue concentration: X₄)

Effect of the process parameters on MB removal

The experimental results showed that the highest MB removal yield (93.35 %) was observed for a NaOH treatment

concentration of 0.1 M, ROS dose in NaOH solutions of 75 g L⁻¹, a stirring time of 1 h, and an initial MB concentration of 60 mg L⁻¹(Table S2). On the other hand, the lowest one (31.03 %) was registered for a NaOH treatment concentration

of 0.06 M, a ROS dose in NaOH solutions of 100 g L^{-1} , a stirring time of 0.5 h, and an initial MB concentration of 120 mg L^{-1} .

The effect of the initial NaOH concentration can be considered as the most influencing variable since the related coefficient is the highest among the studied parameters according to Eq. 8. Moreover, an increase in the concentration of the NaOH enhanced the response of the other parameters in the case of a simultaneous variation (Fig. 2a–c). This could be attributed to the effect that the alkali treatment on the surface of sawdust has changed its morphology and enhanced the concentration of the surface binding sites susceptible to react with MB molecules (Calero et al. 2013).

ROS dose in NaOH solutions was also found to be determinant on the MB removal efficiency during the batch adsorption studies. An augmentation of this stirred dose was noticed to decrease the dye removal yield (Fig. 2e). This is due to the screen effect caused by the sawdust particles in the case of a high biomass treatment, which lowers the chance for lignocellulosic material to be sufficiently exposed to chemical treatment, and abates the amount of OH^- adsorption functional groups to be fixed on the surface (Azzaz et al. 2015). Indeed, high stirring duration achieves better contact between NaOH molecules and sawdust particles, which enhances the chemical properties of the biomass. The highest MB removal efficiencies were observed when increasing stirring times and the NaOH concentrations simultaneously (Fig. 2b). Similarly, a concurrent increase in stirring time and a decrease in ROS dose in NaOH solutions boosted MB uptake up to removal yields of 85 % (Fig. 2d). In an economically speaking point of view, many studies opted for stirring time between 30 and 120 min and suggested that an excess in activation period could alter the lignocellulosic material and decrease their ability for pollutant retention (Pavlović et al. 2014).

Optimization using desirability function

Optimal conditions for MB removal from aqueous solutions onto the alkaline-modified sawdust were assessed with the desirability function (DF) in Minitab V17. This feature was used to determine the optimal conditions for a desired response, based on the second-order polynomial equation. The lower ($d = 0$ designing the response at its undesirable limit) and the upper ($d = 1.0$ designing a very desirable limit of the response) were fixed to assure a total coverage to the parameter variations (Gomes et al. 2016). The optimal design suggests that the maximum dye removal (Target = 100 %, for a $d = 1.0$) could be achieved for the following experimental conditions: NaOH concentration of 0.14 M, a treated adsorbent dosage of 50 g L^{-1} , a stirring time of 1 h, and an MB concentration of 69.5 mg L^{-1} (Fig. S1).

To ensure the validation of the model and to confirm the desired fit between experimental and theoretical data, an experiment at the previously cited conditions was performed and

the results showed an MB removal yield of 95.34 %. With such difference (lower than 5 %), the elaborated model could be considered as valid. Similar findings were recorded in literature (Ghaedi et al. 2015; Gomes et al. 2016; Tehrani and Zare-Dorabei 2016; Pavlović et al. 2014).

Morphological, physical, and chemical characterization of raw and modified sawdust

The particle size distribution analysis of ROS and ATOS indicated that they could be considered both as heterogeneous media since their uniformity coefficients were higher than 2 (Table 3). They are also medium to coarse porous media since their mean diameters (d_{50}) were estimated to be 0.593 and 0.736 mm, respectively. The chemical treatment has significantly reduced the percentage of the fraction having small size. This finding could be attributed to the disintegration of the lignin matrix and a possible conglomeration between the small fractions. The TGA curves (Fig. S2 and S3) showed that the modification with NaOH has decreased the orange tree sawdust's moisture (up to $120 \text{ }^\circ\text{C}$) from 8.88 to 7.26 %. This decrease is due to the drying step, performed prior the alkali treatment of the sawdust (Calero et al. 2013). The alkaline treatment has also dropped hemicellulose and lignin contents from 23.5 to 20.6 % and from 18.7 to 11.8 %, respectively (Fig. S2 and S3). This finding could be attributed to the hydrolysis reactions occurring during the biomass treatment. Similar finding has been reported by Calero et al. (2013) when investigating olive tree pruning modification by NaOH. Nonetheless, the performed alkali treatment has increased the cellulose content from 48.9 to 60.3 % (Table 3). According to Rahman et al. (2005), sawdust treatment with NaOH solution converted the ester groups of cellulose I, hemicellulose, and lignin into carboxylate ligands characterizing cellulose II as a thermodynamically more stable component. Similar results were found by Vadivelan and Vasanth Kumar (2005), when investigating the alkali treatment of rice husk.

To assess the possible physical modifications affecting the surface of the sawdust surface induced by the chemical treatment, spectroscopic imagery and mineral elemental composition analyses were performed using SEM coupled with EDS (Fig. 3). SEM analysis showed an important modification on the surface of the biomass after the chemical treatment. Both biomasses were characterized with rough morphology and presented an important number of pores, cracks, and cavities. However, modified sawdust showed wider voids and kinks due to the scouring process of lipids, cellulose, and hemicellulose and the rearrangement of their crystallography. In addition, the chemical modification has significantly changed the elementary composition of the sawdust surface. Indeed, the EDS analyses revealed the appearance of an important new peak corresponding to the fixation of Na^+ during the treatment with NaOH. Johar et al. (2012) pointed out that sodium ions,

characterized with their small atomic radius (1.8 to 1.9 Å) could easily slide into the inner sawdust structure, which allows its incorporation with the phenolic and carboxylic functional groups and consequently could enhance the ion exchange process during the adsorption of MB molecules.

On the other hand, according to Jiang et al. (2013), the alkali treatment affected the structure of the biomass and shifted the crystallographic arrangement of its components. In fact, NaOH molecules caused the swelling of the lignocellulosic matrix, accompanied by the removal of minerals that existed in the pore structure. The demineralization process entrained the widening of the pores. This observation was confirmed by the XRD diagrams (Fig. 4) where three diffraction peaks were registered for ROS at $2\theta = 15.1^\circ$, 22.6° , and 26.2° corresponding to (110), (101), and (002) crystal planes, respectively. These peaks are typically related to the cellulose I structure (Wang 2013). After the alkali treatment, two other peaks appeared at $2\theta = 16.2^\circ$ and 24.1° , which could be assigned to the (1–10), (110), and (020) crystal planes of cellulose II (Shi et al. 2014). The cellulose matrix showed a swelling efficiency in the NaOH solvent at low temperature which resulted in some molecular mobility that led to the transformation from cellulose I to cellulose II (French 2014). The modification of holocellulosic crystallography presented a more stable structure characterized with a low value of free energy (Gwon et al. 2010).

Since the adsorption of a given ion or molecule onto an organic material depends mainly on the acidic or basic oxygen groups present on its surface (Boehm 2002), it is important to have a precise idea on the functional chemical groups present

on the surface of both studied biomass. For this purpose, Boehm titration was performed for ROS and ATOS and the results are gathered in Table 3. The effect of NaOH treatment was observed mainly on the amounts of hydroxyl groups that increased from about 2.768 to 3.401 mmol g⁻¹ (Table 3). Raw sawdust presented higher amount of surface acidic groups (2.965 mmol g⁻¹) than did the one found for the treated biomass. However, the alkali treatment changed the electronic aspect of the sawdust surface by decreasing the amount of acidic groups by 42 % (1.710 mmol g⁻¹) and increasing the amount of hydroxyl groups by about 21 %. Furthermore, the NaOH treatment decreased the amount of carboxylic and lactonic groups (Table 3), indicating an important modification in the outer structure of the surface. It suggests a possible alteration process of the cellulose and hemicellulose matrix that induced the decomposition of the rigid structure surrounding the biomass and neutralizing their characterizing functional groups. Yet, phenolic groups increased by about 11 % after the alkali treatment. According to Wan Ngah and Hanafiah (2008), a treatment of lignocellulosic material with alkali solution enhanced the amount of polyphenolic groups which could cause the swelling of the wooden fibers and augment the probability of OH⁻ groups fixation onto their surface. These results are in concordance with previous studies (Wan Ngah and Hanafiah 2008; Calero et al. 2013).

The pH_{zpc} values of the ROS and ATOS were evaluated to 5.70 and 8.05, respectively, which confirm the Boehm titration results. This result upholds also the fact that before treatment, raw sawdust was characterized with a slightly acidic surface, dominated mainly by phenolic, carboxylic, and lactonic groups. When increasing pH values, and at the presence of high concentrations of hydroxyl ions, these groups were deprotonated and the surface becomes negatively charged.

Table 3 Main physicochemical characteristics of the used adsorbents (ROS: raw orange tree sawdust; ATOS: alkali-treated orange tree sawdust; d_x: mesh diameter that allows x% of the lignocellulosic material to pass through; 2: UC: uniformity coefficient: ratio of d₆₀/d₁₀; pH_{zpc}: pH at zero-point charge)

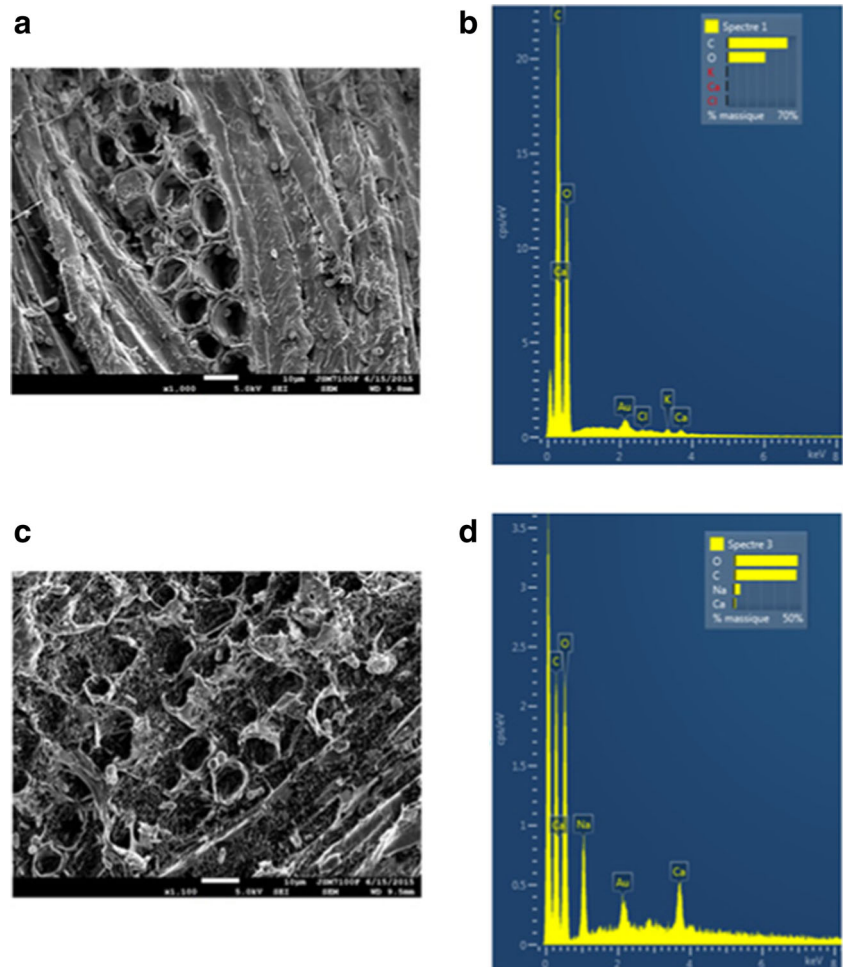
Properties		ROS	ATOS
Grain size distribution	d ₁₀	0.100	0.297
	d ₅₀	0.593	0.736
	d ₆₀	0.771	0.802
	UC	7.712	2.700
Composition (%)	Moisture	8.88	7.26
	Holocellulose	72.4	80.92
	α-cellulose	48.9	60.32
	Hemicellulose	23.5	20.60
	Lignin	18.72	11.82
Boehm titration (mmol g ⁻¹)	Carboxylic	2.450	1.471
	Lactonic	0.433	0.148
	Phenolic	0.082	0.091
	Hydroxyl	2.768	3.401
Charges density	pH _{zpc}	5.70	8.05

MB removal studies

Kinetic studies

In order to determine the removal rate of MB from aqueous solutions by ROS and ATOS, a kinetic study was performed for contact times varying from 1 to 240 min. As presented in Fig. 5, the non-linear process of adsorption through time shows that MB uptake is occurring by means of a multitude of mechanisms and steps. The adsorbed MB quantity increased quickly at the first 40 min of contact, reaching a removal yield of 71 and 79 % of the total amount of adsorbed dye for ROS and ATOS at equilibrium, respectively. This fast adsorption rate is due to the abundant presence of MB molecules as well as free acidic functional groups on both adsorbents (Akrouf et al. 2015; Azzaz et al. 2015). Later, MB uptake rate slowed and the adsorption curve presented a less stiffened slope. This observation suggests a possible MB diffusion through biomass caused by the saturation of the surface

Fig. 3 SEM imaging and EDS for raw (a, b) and alkali modified (c, d) sawdust



sites. Complete saturation was then reached for both adsorbents at 180 min of contact time. It is worth mentioning that MB removal efficiency at equilibrium for ATOS has almost doubled compared to the one observed for ROS. This is attributed to the alkali attack that affected the chemical composition of the sawdust surface by generating more O-Na sites

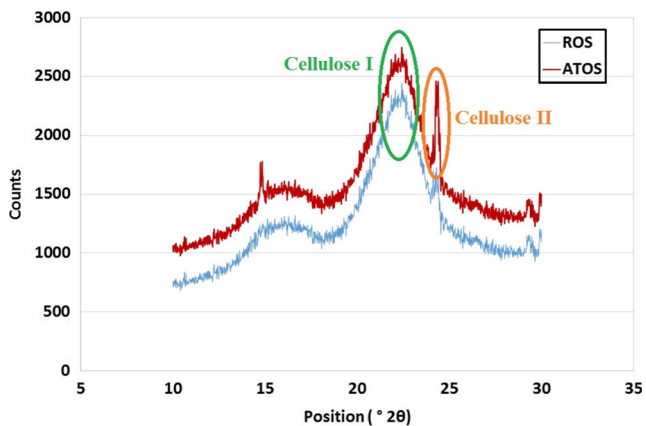


Fig. 4 XRD of raw (ROS) and modified (ATOS) sawdust

that could bind with dye molecules. Similar results were reported by Gwon et al. (2010).

The used kinetic models presented high correlation coefficients and indicated a good fit to the experimental data

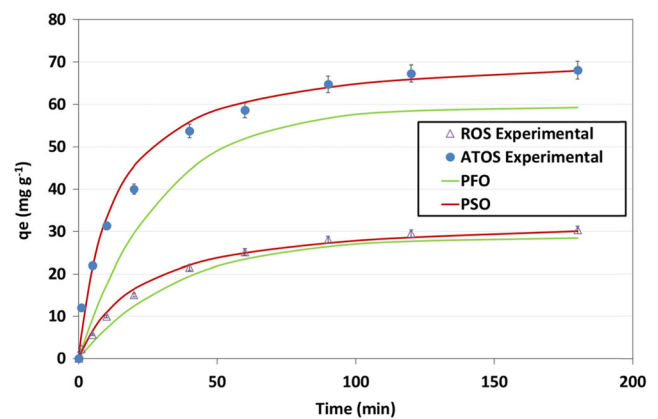


Fig. 5 MB kinetic adsorption onto ROS and ATOS and their fitting by pseudo-first-order and pseudo-second-order kinetic models ($C_0 = 69.5 \text{ mg L}^{-1}$, pH 6.0, adsorbent dose = 1 g L^{-1} , temperature = $20 \pm 2 \text{ }^\circ\text{C}$)

Table 4 Kinetic parameters for MB adsorption onto ROS and ATOS ($C_0 = 69.5 \text{ mg L}^{-1}$, pH 6.0, dose = 1 g L^{-1} , temperature = $20 \pm 2 \text{ }^\circ\text{C}$, $q_{e,exp}$: MB adsorbed quantity at equilibrium)

	Pseudo-first order					Pseudo-second order				Film diffusion		Intraparticle diffusion	
	$q_{e,exp}$ (mg g^{-1})	k_1 (min^{-1})	$q_{e,1}$ (mg g^{-1})	R^2	APE (%)	k_2 (g $\text{mg}^{-1} \text{ min}^{-1}$)	$q_{e,II}$ (mg g^{-1})	R^2	APE (%)	D_f ($\text{m}^2 \text{ s}^{-1}$)	R^2	D_{ip} ($\text{m}^2 \text{ s}^{-1}$)	R^2
ROS	30.145	0.0285	28.641	0.998	19.673	0.00143	33.557	0.997	8.794	8.186 E-10	0.987	3.044 E-10	0.998
ATOS	68.079	0.0345	59.401	0.989	30.910	0.00116	72.463	0.997	9.526	2.034 E-09	0.983	8.507 E-10	0.976

(Table 4). However, for the pseudo-first-order model, the theoretical adsorbed amount of MB at equilibrium ($q_{e, cal}$) did not fit well the experimental data for both adsorbents and suggested that adsorption was not conducted through a pseudo-first-order (PFO) process. On the other hand, the theoretical amount of MB uptake using the pseudo-second-order model (PSO) was more adequate to experimental data. In addition, the corresponding calculated APE values were lower compared to the ones of the PFO results. Thereby, the pseudo-second-order model was found to be more suitable to predict the experimental data for both ROS and ATOS. This finding indicates that MB removal from aqueous solution might be mainly governed by a chemisorption process, with the establishment of strong electronic bonding between dye molecules and the surface functional sites. Analogous findings were reported by Bouaziz et al. (2014), when studying the removal of MB by softwood sawdust.

The analysis of the adsorption of MB onto the ROS and ATOS with film and intraparticle diffusion models showed that the adsorption process was driven by a surface adsorption at earlier stages (up to 40 min of contact) followed by

intraparticle diffusion until reaching equilibrium. The values of diffusion coefficients given in Table 4 indicate that intraparticle diffusion coefficients are about 2.7 and 2.4 times lower than those of the film diffusion through the limit layer for ROS and ATOS, respectively. This finding confirms that in the case of the tested adsorbents, the intraparticle diffusion process controls significantly the rate of adsorption of MB ions. Similar outcomes have been observed in other studies (Azzaz et al. 2015).

It is worth mentioning that final pH was measured for MB adsorption experiments onto both ROS and ATOS. Final pH values showed an insignificant modification in the bulk pH in the case of dye uptake onto the raw material, since its pH_{zpc} is close to the natural pH. However, for MB removal by ATOS, at equilibrium, the final solution pH values increased from 6.0 to an average value of 7.95. This finding is attributed to the high concentrations of negatively charged hydroxyl groups present on the surface of ATOS. These fixation sites bond with the cations initially present in the bulk solution (mainly H^+ , MB), which reduces their concentrations and increases the solution pH, until they reach values that are relatively close to ATOS pH_{zpc} . Similar findings were reported by Annadurai et al. (2002) when he studied the removal of methylene blue by orange and banana peels.

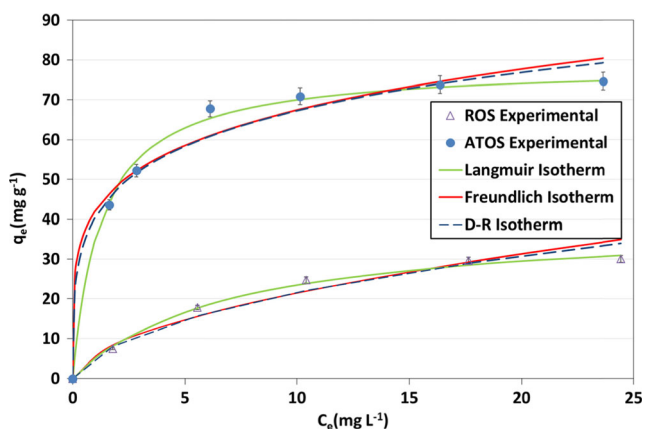


Fig. 6 MB adsorption onto ATOS and ROS at equilibrium and their fitting by Langmuir, Freundlich, and D-R isotherm models ($C_{0,ROS} = 10\text{--}50 \text{ mg L}^{-1}$, $C_{0,ATOS} = 40\text{--}100 \text{ mg L}^{-1}$, contact time = 3 h, pH 6.0, adsorbent dose in MB solutions = 1 g/L , temperature = $20 \pm 2 \text{ }^\circ\text{C}$)

Effect of initial MB concentrations: isotherm modeling

Results indicated that MB uptake increased with increasing initial concentration. Indeed, the removed MB amounts varied from 8.1 to 31 mg g^{-1} for ROS and from 43.5 to 74.6 mg g^{-1} for ATOS when those for the MB aqueous concentrations increased from 10 to 50 mg L^{-1} and from 40 to 100 mg L^{-1} , respectively (Fig. 6). This finding suggests that an increase in initial MB concentrations causes an increase in the concentration gradient between the solid and aqueous phases which enhances dye molecule diffusion rate through the used biomasses.

These found experimental data were fitted to the Langmuir, Freundlich, and Dubinin–Radushkevich (D-R) models

Table 5 MB adsorption onto ATOS and ROS at equilibrium and their fitting by Langmuir, Freundlich, and D–R isotherm models ($C_{0-ROS} = 10\text{--}50 \text{ mg L}^{-1}$, $C_{0-ATOS} = 40\text{--}100 \text{ mg L}^{-1}$, contact time = 3 h, pH 6.0, dose = 1 g L^{-1} , temperature = $20 \pm 2 \text{ }^\circ\text{C}$)

	Langmuir				Freundlich				Dubinin–Radushkevich (D–R)				
	q_{\max} (mg g^{-1})	K_L (L mg^{-1})	E (kJ mol^{-1})	R^2	APE (%)	n	K_F ($\text{mg}^{-1(1/n)}$ $\text{L}^{(1/n)} \text{g}^{-1}$)	R^2	APE (%)	q_m (mg g^{-1})	E (kJ mol^{-1})	R^2	APE (%)
ROS	39.683	5.377	10.783	0.992	4.009	1.835	6.119	0.949	10.764	336.505	10.783	0.963	9.168
ATOS	78.74	0.798	17.584	0.999	2.107	4.892	42.127	0.904	5.049	188.88	17.584	0.923	4.500

(Table 5 and Fig. 6). The highest values of correlation coefficients ($R^2 = 0.992$ and 0.999) and lowest APE (4.009 and 2.107 %) corresponded to the Langmuir model for both ROS and ATOS, respectively. Thereby, MB adsorption onto ROS and ATOS was considered as a monolayer fixation process characterized with uniform functional site occupation by dye molecules at constant energy (Rafatullah et al. 2010). Furthermore, Langmuir coefficient values ($R_L = \frac{1}{1+K_L c_0}$) were between 0.122 and 0.409 for ROS and between 0.03 and 0.123 for ATOS, respectively, indicating a favorable MB adsorption process by both materials. Regarding the Freundlich model, the calculated determination coefficients and APE were less fitting to the experimental data and higher than the values found for the Langmuir model, which excludes the assumption of a possible non-uniform adsorption of dye onto a heterogeneous surface. Calculated Freundlich parameter “ n ” was estimated to be 1.835 and 4.892 for ROS and ATOS, respectively, which belong to the range of 1–10, indicating a favorable adsorption of MB onto the two tested adsorbents. On the other hand, the calculus of the free energy (E) by the D–R model which reflects the adsorption tendency whether it is a physisorption ($E < 8 \text{ kJ mol}^{-1}$) or a chemisorption ($E > 8 \text{ kJ mol}^{-1}$) process confirms that MB removal by both ROS and ATOS was mainly chemical (Table 5). However, the estimated R^2 (0.963 and 0.923), APE (9.168 and 4.5 %) and theoretical maximal adsorption capacity

(336.5 and 188.88 mg g^{-1}) for ROS and ATOS, respectively, did not fit well the experimental data (Table 5). Pezoti Junior et al. (2014) found comparable results when studying methylene blue removal by ZnCl_2 -activated carbon.

In order to situate the efficiencies of ROS and ATOS in removing MB from aqueous solutions, a comparison of their “ q_e ” with several lignocellulosic adsorbents was carried out (Table 6). It appears that ATOS presents a relatively high MB removal capacity compared to alkali-treated neem leaf powder and orange peel (Annadurai et al. 2002; Bhattacharya and Sharma 2005). On the other hand, dye removal efficiency by ATOS was found to be globally similar to the one recorded for the garlic peels (Hameed and Ahmad 2009). These results confirm that ATOS could be considered as an interesting low-cost material for the removal of dyes from aqueous solutions.

pH effect

The effect of the surrounding pH on the MB adsorption onto ROS and ATOS was followed for initial values of 3, 5, 6, 9, and 11. The experimental results (Fig. 7) indicated that MB removal efficiencies significantly increased when increasing initial solution pH values. For instance, for ROS, the estimated MB removal yield rose from 24.2 to 58.9 % for initial pH values of 3 and 11, respectively. The relatively low MB

Table 6 Comparison of MB adsorption onto ROS and ATOS with other organic adsorbents

Material	C_0 (mg L^{-1})	Adsorption capacity (mg g^{-1})	Reference
NaHCO_3 neem leaf powder	25–70	3.67	Bhattacharya and Sharma (2005)
Activated date pits	20–400	12.9	Banat et al. (2003)
NaOH-treated coconut coir	60–100	15.59	Sharma and Upadhyay (2009)
Orange peel	20–60	18.6	Annadurai et al. (2002)
Wood apple rind-carbon	20–100	40.00	Malarvizhi and Ho (2010)
NaOH-treated rice husk	10–125	40.58	Vadivelan and Vasanth Kumar (2005)
Garlic peel	25–200	82.64	Hameed and Ahmad (2009)
Raw orange tree sawdust	10–50	39.68	This study
Alkali-treated orange tree sawdust	40–100	78.74	This study

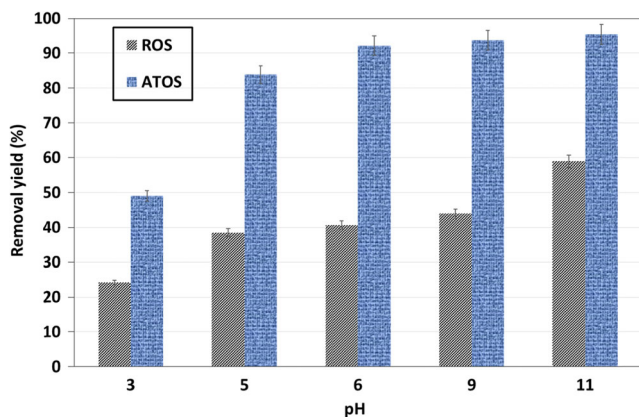


Fig. 7 Effect of pH on the MB removal at equilibrium by ROS and ATOS ($C_0 = 69.5 \text{ mg L}^{-1}$, adsorbent dose = 1 g L^{-1} , temperature = $20 \pm 2 \text{ }^\circ\text{C}$)

removal efficiencies observed at lower pH values were due to the competition effect between dye molecules and free proton bonding with surface groups. In fact, in the case of a surrounding solution pH under the value of pH_{zpc} biomass, the surface is mainly positively charged and a repulsion phenomenon between the dye molecules and the cationic surface groups occurs, which causes a limitation of MB uptake. However, at $\text{pH} > \text{pH}_{\text{zpc}}$, the deprotonated surface groups were more likely to fix higher amounts of the cationic dye molecules due to the increasing amount of negatively functional sites (Jellali et al. 2011a). These findings confirm that MB uptake onto both raw and modified orange sawdust was governed by chemisorption reactions. Similar results were reported for MB removal by pine tree leaves (Yagub et al. 2012).

Adsorption mechanism investigations

Ion exchange mechanism during the adsorption process was investigated in batch mode for the major cation release in

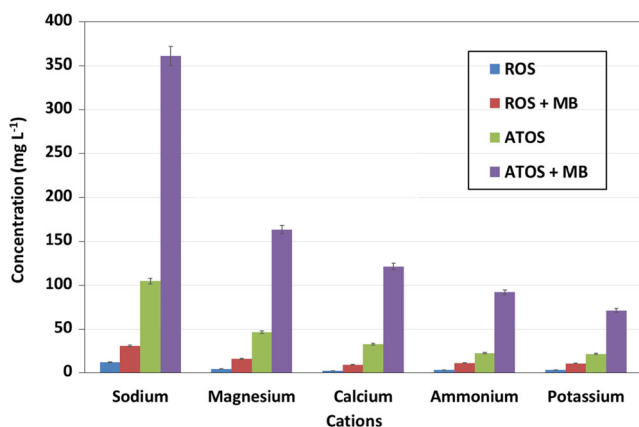


Fig. 8 Cation exchange assessment for blank (without MB) and dye solutions ($C_0 = 69.5 \text{ mg L}^{-1}$, contact time = 3 h, pH = 6.0, adsorbent dose = 1 g L^{-1} , temperature = $20 \pm 2 \text{ }^\circ\text{C}$)

aqueous solutions for both raw and alkali-modified orange tree sawdust. Results (Fig. 8) showed that for blank experiments, cationic release significantly increased after alkali treatment. Indeed, the total released cations increased from about 25.5 mg L^{-1} for ROS to 228.6 mg L^{-1} for ATOS. Maximum increase was imputed to the sodium cations where their concentrations rose from 12.2 for ROS to 105.2 mg L^{-1} for ATOS. This behavior is due to the effect of alkali treatment on the mineral composition of the biomass, characterized by the scouring of its outer crust and the fixation of Na^+ ions on the functional acidic groups (Azzaz et al. 2015).

On the other hand, the presence of MB has increased the total released cations by about 207.9 and 253.8 % compared to the ones registered for the blank experiments for ROS and ATOS, respectively. Maximum released concentrations were observed for sodium and magnesium cations, which increased by about 18.6 and 11.8 mg L^{-1} for ROS and 255.6 and 116.7 mg L^{-1} for ATOS, respectively. This rise in ionic concentration was caused by the increase of the mass transfer of dye molecules from liquid to solid phase, enhancing the liberation of cations from the biomasses. These outcomes highlight the importance of proton donor sites which were involved in the ion exchange process by a possible deprotonation in the presence of the dye molecules. This finding has been reported by Amirmia et al. (2016) when studying the removal of copper ions using maple leaves in continuous-flow column.

It is worth mentioning that MB adsorption process would be a combination of cationic exchange mechanism and complexation through surface functional sites containing free electrons. The latter has been pointed out by several authors as an important mechanism during cationic dye adsorption process by lignocellulosic materials. For instance, Djilali et al. (2012) demonstrated that the main functional groups involved in the adsorption of MB by modified timber sawdust were carboxylic and carbonyl groups. Besides these functional groups, Sen et al. (2011) showed that MB removal by pine cone biomass through complexation mechanism included also hydroxyl, ester, and aliphatic groups.

Effect of the presence of metal ions in dye solution

Results gathered in Fig. 9 showed that adsorption of MB decreased in the presence of metal ions. In fact, the adsorbed MB amount decreased from 68.08 mg g^{-1} (in absence of Zn(II)) to 46.4 mg g^{-1} when the used zinc concentration was fixed to 140 mg L^{-1} . Furthermore, it has been found that relatively high amounts of Zn(II) have been simultaneously removed by ATOS. In fact, for an initial Zn(II) concentration of 140 mg L^{-1} , its removal capacity reached about 32.5 mg g^{-1} . This finding is attributed to the fact that Zn(II) ions have a small atomic radius (1.35 to 1.42 \AA), which allows it to be easily incorporated through the cellulose II matrix, as

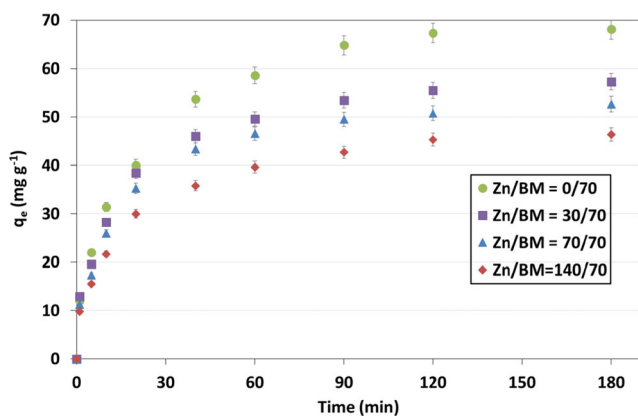


Fig. 9 MB kinetic adsorption onto ATOS in presence of Zn(II) ($C_{MB} = 69.5 \text{ mg L}^{-1}$, $\text{pH} = 6.0$, adsorbent dose in MB solutions = 1 g L^{-1} , temperature = $20 \pm 2 \text{ }^\circ\text{C}$)

well as to occupy surface functional groups, entering thereby in competition with relatively big MB molecules. Kinetic modeling through pseudo-first-order and pseudo-second-order models (data not shown) confirmed that the latter model fitted the best the experimental data, which indicated that adsorption of MB onto sawdust remained mainly a chemisorption process despite the presence of metals in the solution. Similar results were reported by Kyzas et al. (2015) when studying the simultaneous removal of Remarcyl Red and zinc from aqueous solution by succinyl-grafted chitosan.

Desorption experiments

Dye desorption experiments were elaborated and the related results are presented in Fig. 10. For both ROS and ATOS adsorbents, the MB desorption efficiency was found to increase when increasing NaCl concentrations from 0.05 to 1 M. For instance, the MB desorption efficiency from ROS increased from about 35.5 to 65.8 % when increasing salt

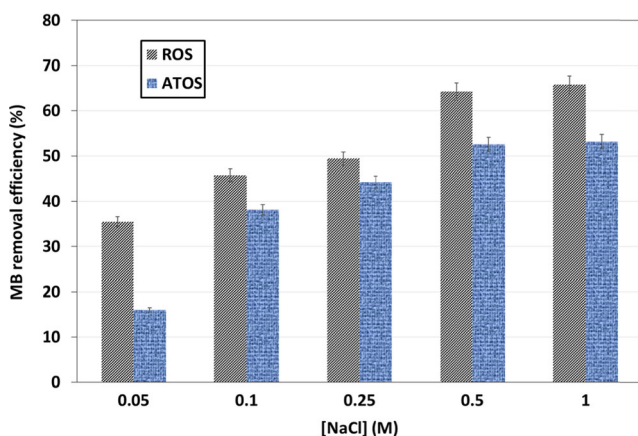


Fig. 10 Effect of initial NaCl concentration on MB desorption from ROS and ATOS (adsorbent dose in distilled water = 1 g L^{-1} , contact time = 2 h, temperature = $20 \pm 2 \text{ }^\circ\text{C}$)

concentration from 0.05 to 1 M, respectively. The same tendency was observed for ATOS, with a calculated dye desorption going from about 16.0 to 53.2 % for the same NaCl concentration variation range. These were found relatively low MB desorption capacities compared to other studies (Djilali et al. 2012) and could be imputed to the biomasses' surface characteristics, which present important amounts of highly binding functional groups, making the desorption process more difficult (Azzaz et al. 2015). The MB desorption could be mainly imputed to the ion exchange phenomenon that occurs between dye molecules already fixed on the biomass and the abundant sodium ions. These findings suggest a possible regeneration of both adsorbents and an eventual recovery of dye for further industrial use. Similar findings were pointed out by Malekbala et al. (2015), when studying the adsorption/desorption of MB onto ceramic monoliths using NaCl solutions.

Conclusions

This study investigated the optimization of the alkali treatment of orange tree sawdust process for methylene blue removal from aqueous solutions in batch mode, by using a rotatable central composite design of experiment. Results showed that the NaOH treatment concentration ($[\text{NaOH}]_{\text{Optimal}} = 0.14 \text{ M}$) as well as the contact time ($T_{\text{Optimal}} = 60 \text{ min}$) were the most influential parameters that effect the dye efficiency uptake by the modified sawdust. Furthermore, the found model fitted very well the experimental results with high determination coefficients ($R^2 = 0.973$ and adjusted $R^2 = 0.955$). The treated sawdust has undergone very important morphological, physical, and chemical modifications, characterized with a noticeable increase in the quantity of hydroxyl groups by 21 % and decrease in the amount of acidic groups by 42 %, which indicates the shifting of electronic properties of the ATOS for a better adsorption of MB molecules. Kinetic data indicated that MB adsorption onto raw and modified sawdust was well fitted with the pseudo-second-order model, suggesting the presence of a chemisorption process. Moreover, isotherm studies showed that the Langmuir model suits the best the experimental data, indicating that MB removal onto ATOS is a monolayer adsorption. The maximal theoretical adsorption MB quantity was estimated to be 78.74 mg g^{-1} , which is relatively important compared to previous studies. Ionic chromatography analyses of blank and MB aqueous solution samples showed that the main involved mechanisms during MB adsorption onto raw and ATOS involve not only electronic bonding through free electron sites but also a cationic exchange process. Combined pollution with Zn(II) showed that ATOS presents important capacity in removing simultaneously dyes and heavy metals. Desorption experiments by using NaCl solutions presented a recovering efficiency of 65.8 and

53.2 %, for ROS and ATOS, respectively. This suggests a possible reuse of these biomasses for further adsorption applications. Further investigations are currently undertaken regarding the assessment of MB adsorption and desorption by the modified biomass in fixed bed column systems under various experimental conditions.

Acknowledgments This research work has been carried out in the framework of a Tunisian national project. Financial support of this work by the Tunisian Ministry of Higher Education and Scientific Research is gratefully acknowledged.

References

- Akrout H, Jellali S, Bousselmi L (2015) Enhancement of methylene blue removal by anodic oxidation using BDD electrode combined with adsorption onto sawdust. *Comptes Rendus Chim* 18:110–120. doi:10.1016/j.crci.2014.09.006
- Al Jibouri AKH, Wu J, Upreti SR (2015) Continuous ozonation of methylene blue in water. *J water. Process Eng* 8:142–150. doi:10.1016/j.jwpe.2015.10.002
- Amirnia S, Ray MB, Margaritis A (2016) Copper ion removal by *Acer saccharum* leaves in a regenerable continuous-flow column. *Chem Eng J* 287:755–764. doi:10.1016/j.cej.2015.11.056
- Annadurai G, Juang RS, Lee DJ (2002) Use of cellulose-based wastes for adsorption of dyes from aqueous solutions. *J Hazard Mater* 92:263–274. doi:10.1016/S0304-3894(02)00017-1
- Azzaz AA, Jellali S, Assadi AA, Bousselmi L (2015) Chemical treatment of orange tree sawdust for a cationic dye enhancement removal from aqueous solutions: kinetic, equilibrium and thermodynamic studies. *Desalin Water Treat* 3994:1–13. doi:10.1080/19443994.2015.1103313
- Banat F, Al-Asheh S, Al-Makhadmeh L (2003) Evaluation of the use of raw and activated date pits as potential adsorbents for dye containing waters. *Process Biochem* 39:193–202. doi:10.1016/S0032-9592(03)00065-7
- Batzias FA, Sidiras DK (2007) Simulation of methylene blue adsorption by salts-treated beech sawdust in batch and fixed-bed systems. *J Hazard Mater* 149:8–17. doi:10.1016/j.jhazmat.2007.03.043
- Bhattacharya KG, Sharma A (2005) Kinetics and thermodynamics of methylene blue adsorption on neem (*Azadirachta indica*) leaf powder. *Dyes Pigments* 65:51–59. doi:10.1016/j.dyepig.2004.06.016
- Boehm HP (2002) Surface oxides on carbon and their analysis: a critical assessment. *Carbon N Y* 40:145–149. doi:10.1016/S0008-6223(01)00165-8
- Bouaziz I, Chiron C, Abdelhedi R, Savall A, Serrano KG (2014) Treatment of dilute methylene blue-containing wastewater by coupling sawdust adsorption and electrochemical regeneration. *Environ Sci Pollut Res* 21:8565–8572. doi:10.1007/s11356-014-2785-z
- Calero M, Ronda A, Martín-Lara MA, Pérez A, Blázquez G (2013) Chemical activation of olive tree pruning to remove lead(II) in batch system: factorial design for process optimization. *Biomass Bioenergy* 58:322–332. doi:10.1016/j.biombioe.2013.08.021
- Das P, Banerjee P, Mondal S (2014) Mathematical modelling and optimization of synthetic textile dye removal using soil composites as highly competent liner material. *Environ Sci Pollut Res Int*:1318–1328. doi:10.1007/s11356-014-3419-1
- Ding F, Xie Y, Peng W, Peng Y-K (2016) Measuring the bioactivity and molecular conformation of typically globular proteins with phenothiazine-derived methylene blue in solid and in solution: a comparative study using photochemistry and computational chemistry. *J Photochem Photobiol B Biol* 158:69–80. doi:10.1016/j.jphotobiol.2016.02.029
- Djilali, Y, Elandaloussi, EH, Aziz, A, de Ménorval, LC (2012) Alkaline treatment of timber sawdust: a straightforward route toward effective low-cost adsorbent for the enhanced removal of basic dyes from aqueous solutions. *J. Saudi Chem. Soc.*
- French AD (2014) Idealized powder diffraction patterns for cellulose polymorphs. *Cellulose* 21:885–896. doi:10.1007/s10570-013-0030-4
- Ghaedi M, Mazaheri H, Khodadoust S, Hajati S, Purkait MK (2015) Application of central composite design for simultaneous removal of methylene blue and Pb²⁺ ions by walnut wood activated carbon. *Spectrochim Acta—Part A Mol Biomol Spectrosc* 135:479–490. doi:10.1016/j.saa.2014.06.138
- Gomes CS, Piccin JS, Gutterres M (2016) Optimizing adsorption parameters in tannery-dye-containing effluent treatment with leather shaving waste. *Process Saf Environ Prot* 99:98–106. doi:10.1016/j.psep.2015.10.013
- Gwon JG, Lee SY, Doh GH, Kim JH (2010) Characterization of chemically modified wood fibers using FTIR spectroscopy for bio-composites. *J Appl Polym Sci* 116:3212–3219. doi:10.1002/app.31746
- Hameed BH, Ahmad AA (2009) Batch adsorption of methylene blue from aqueous solution by garlic peel, an agricultural waste biomass. *J Hazard Mater* 164:870–875. doi:10.1016/j.jhazmat.2008.08.084
- Jellali S, Ali M, Anane M, Riahi K, Jedidi N (2011a) Biosorption characteristics of ammonium from aqueous solutions onto *Posidonia oceanica* (L.) fibers. *DES* 270:40–49. doi:10.1016/j.desal.2010.11.018
- Jellali S, Ali M, Ben Hassine R, Hamzaoui AH, Bousselmi L (2011b) Adsorption characteristics of phosphorus from aqueous solutions onto phosphate mine wastes. *Chem Eng J* 169:157–165. doi:10.1016/j.cej.2011.02.076
- Jellali S, Diamantopoulos E, Haddad K, Anane M, Durner W, Mlayah A (2016) Lead removal from aqueous solutions by raw sawdust and magnesium pretreated biochar: experimental investigations and numerical modelling. *J Environ Manag* 180:439–449. doi:10.1016/j.jenvman.2016.05.055
- Jiang L, Hu S, Sun LS, Su S, Xu K, He L, Xiang J (2013) Influence of different demineralization treatments on physicochemical structure and thermal degradation of biomass. *Bioresour Technol* 146:254–260. doi:10.1016/j.biortech.2013.07.063
- Johar N, Ahmad I, Dufresne A (2012) Extraction, preparation and characterization of cellulose fibres and nanocrystals from rice husk. *Ind Crop Prod* 37:93–99. doi:10.1016/j.indcrop.2011.12.016
- Kalavathy MH, Regupathi I, Pillai MG, Miranda LR (2009) Modelling, analysis and optimization of adsorption parameters for H₃PO₄ activated rubber wood sawdust using response surface methodology (RSM). *Colloids Surfaces B Biointerfaces* 70:35–45. doi:10.1016/j.colsurfb.2008.12.007
- Kyzas GZ, Sifafa PI, Pavlidou EG, Chrissafis KJ, Bikiaris DN (2015) Synthesis and adsorption application of succinyl-grafted chitosan for the simultaneous removal of zinc and cationic dye from binary hazardous mixtures. *Chem Eng J* 259:438–448. doi:10.1016/j.cej.2014.08.019
- Malarvizhi R, Ho Y-S (2010) The influence of pH and the structure of the dye molecules on adsorption isotherm modeling using activated carbon. *Desalination* 264:97–101. doi:10.1016/j.desal.2010.07.010
- Malekbala MR, Khan MA, Hosseini S, Abdullah LC, Choong TSY (2015) Adsorption/desorption of cationic dye on surfactant modified mesoporous carbon coated monolith: equilibrium, kinetic and thermodynamic studies. *J Ind Eng Chem* 21:369–377. doi:10.1016/j.jiec.2014.02.047
- Nazari G, Abolghasemi H, Esmaili M, Pouya ES (2016) Aqueous phase adsorption of cephalixin by walnut shell-based activated carbon: a fixed-bed column study. *Appl Surf Sci*. doi:10.1016/j.apsusc.2016.03.096
- Pavlović MD, Buntić AV, Mihajlovski KR, Šiler-Marinković SS, Antonović DG, Radovanović Ž, Dimitrijević-Branković SI (2014) Rapid cationic dye adsorption on polyphenol-extracted coffee grounds—a response

- surface methodology approach. *J Taiwan Inst Chem Eng* 45:1691–1699. doi:10.1016/j.jtice.2013.12.018
- Pezoti Junior O, Cazetta AL, Gomes RC et al (2014) Synthesis of ZnCl₂-activated carbon from macadamia nut endocarp (*Macadamia integrifolia*) by microwave-assisted pyrolysis: optimization using RSM and methylene blue adsorption. *J Anal Appl Pyrolysis* 105:166–176. doi:10.1016/j.jaap.2013.10.015
- Rafatullah M, Sulaiman O, Hashim R, Ahmad A (2010) Adsorption of methylene blue on low-cost adsorbents: a review. *J Hazard Mater* 177:70–80
- Rahman HU, Shakirullah M, Ahmad I, Shah S, Shah AA (2005) Removal of copper(II) ions from aqueous medium by sawdust of wood. *J Chem Soc Pakistan* 27:233–238
- Sen TK, Afroze S, Ang HM (2011) Equilibrium, kinetics and mechanism of removal of methylene blue from aqueous solution by adsorption onto pine cone biomass of *Pinus radiata*. *Water Air Soil Pollut* 218:499–515. doi:10.1007/s11270-010-0663-y
- Sharma YC, Upadhyay SN (2009) Removal of a cationic dye from wastewaters by adsorption on activated carbon developed from coconut coir. *Energy and Fuels* 23:2983–2988. doi:10.1021/ef900113z
- Shi Z, Yang Q, Cai J (2014) Effects of lignin and hemicellulose contents on dissolution of wood pulp in aqueous NaOH/urea solution. *Cellulose* 21:1205–1215. doi:10.1007/s10570-014-0226-2
- Soniya M, Muthuraman G (2013) Recovery of methylene blue from aqueous solution by liquid–liquid extraction. *Desalin Water Treat*: 1–9. doi:10.1080/19443994.2013.866055
- Tehrani MS, Zare-Dorabei R (2016) Competitive removal of hazardous dyes from aqueous solution by MIL-68(Al): derivative spectrophotometric method and response surface methodology approach. *Spectrochim Acta - Part A Mol Biomol Spectrosc* 160:8–18. doi:10.1016/j.saa.2016.02.002
- Vadivelan V, Vasanth Kumar K (2005) Equilibrium, kinetics, mechanism, and process design for the sorption of methylene blue onto rice husk. *J Colloid Interface Sci* 286:90–100. doi:10.1016/j.jcis.2005.01.007
- Wan Ngah WS, Hanafiah MAKM (2008) Removal of heavy metal ions from wastewater by chemically modified plant wastes as adsorbents: a review. *Bioresour Technol* 99:3935–3948. doi:10.1016/j.biortech.2007.06.011
- Wang L (2013) Removal of disperse red dye by bamboo-based activated carbon: optimisation, kinetics and equilibrium. *Environ Sci Pollut Res* 20:4635–4646. doi:10.1007/s11356-012-1421-z
- Yagub MT, Sen TK, Afroze S, Ang HM (2014) Dye and its removal from aqueous solution by adsorption: a review. *Adv Colloid Interf Sci* 209:172–184. doi:10.1016/j.cis.2014.04.002
- Yagub MT, Sen TK, Ang HM (2012) Equilibrium, kinetics, and thermodynamics of methylene blue adsorption by pine tree leaves. *Water Air Soil Pollut* 223:5267–5282. doi:10.1007/s11270-012-1277-3